LETTERS

Free choice activates a decision circuit between frontal and parietal cortex

Bijan Pesaran[1,3], Matthew J. Nelson[2] & Richard A. Andersen[2,3]

We often face alternatives that we are free to choose between. Planning movements to select an alternative involves several areas in frontal and parietal cortex[1–11] that are anatomically connected into long-range circuits[12]. These areas must coordinate their activity to select a common movement goal, but how neural circuits make decisions remains poorly understood. Here we simultaneously record from the dorsal premotor area (PMd) in frontal cortex and the parietal reach region (PRR) in parietal cortex to investigate neural circuit mechanisms for decision making. We find that correlations in spike and local field potential (LFP) activity between these areas are greater when monkeys are freely making choices than when they are following instructions. We propose that a decision circuit featuring a sub-population of cells in frontal and parietal cortex may exchange information to coordinate activity between these areas. Cells participating in this decision circuit may influence movement choices by providing a common bias to the selection of movement goals.

According to theories of decision making, we make choices by selecting the alternative that is most valuable to us[13]. How much we value each alternative is revealed by our choices. If we value swimming as much as running, we will choose to do both instead of always choosing one over the other. Although actions with similar values can lead to different choices, only one choice can be made at a time. Planning a movement to select an alternative activates many areas of the brain. How does the brain decide what to do? PMd and PRR plan reaching arm movements[14] and are directly connected[12]. We therefore studied these areas to identify a neural circuit for deciding where to reach. We trained two monkeys to do a free search task and an instructed search task (Fig. 1a, b). In both tasks, monkeys made a sequence of reaches to visual targets for rewards of juice. The key manipulation was that, in the free search task, the three targets were visually identical circles, and the monkey could search in any sequence (Fig. 1a); whereas in the instructed search task, the three targets were a circle, a square and a triangle, and the monkey had to search in a fixed sequence (Fig. 1b). To control other sensory, motor and reward-related factors, we carefully matched the two tasks by yoking the sequences presented in the instructed task to the monkey's choices in the free search task (see Methods, Supplementary Results and Supplementary Fig. 2).

During free search, each monkey's choices varied, even for identical stimuli (Fig. 1c). In contrast, instructed search movement sequences did not vary (Fig. 1d). Overall, each monkey developed a free search strategy and chose between two or three different movement sequences for most search arrays (Supplementary Fig. 3).

Although the tasks we studied could differ in other aspects, like reward expectancy, attention or overall effort, analysis of each animal's behaviour indicates that the major difference involves decision making (Supplementary Results). Free and instructed search involve different decisions because the alternatives have different values. Free search involves choosing between movement sequences with similar values so choices vary from trial to trial (Fig. 1c). Because we reward only one movement sequence, instructed search involves alternatives with very different values. Consequently, each monkey repeatedly makes the same choices (Fig. 1d).

When movement choices vary from trial to trial, PMd and PRR must coordinate their activity. Analysing spiking and LFP activity may resolve neural coordination between these areas. Spiking activity measures action potentials from individual neurons. LFP activity predominantly measures synaptic potentials in a population of neurons near the recording electrode[15]. Spike–field coherency directly relates these two signals by measuring how well LFP activity is predicted by action potentials. We therefore measured spike–field coherency to characterize neural coordination between PMd and PRR and identify the neurons involved in this coordination.

We made 314 PMd spike–PRR field and 187 PRR spike–PMd field recordings in two animals during both free and instructed search
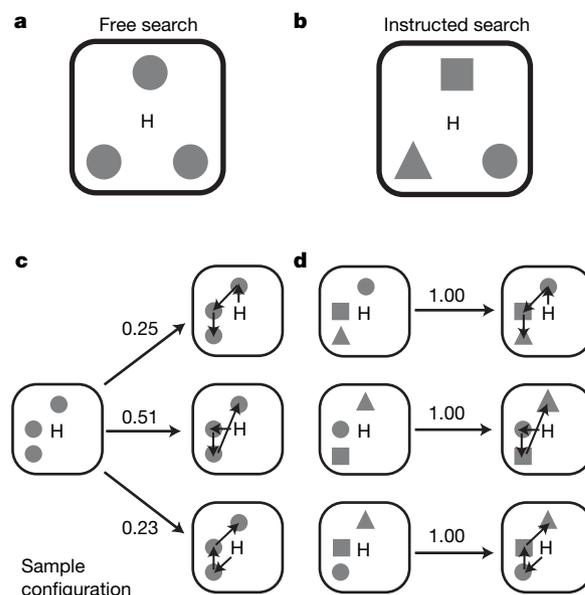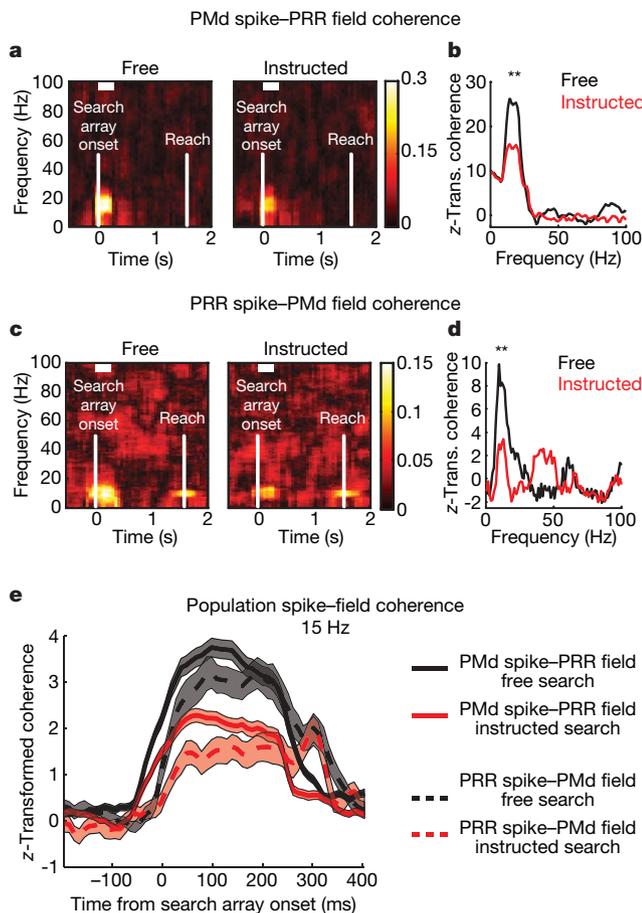

Figure 1 | Task and behaviour. a, Free search task. Three circular targets presented at eight potential locations spaced 10° apart around the central hand position, H. **b,** Instructed search task. Targets in the instructed search task were a circle, square and triangle; the monkey had to reach to them in that order. Each target had an equal, one-third, probability of being the rewarded target. **c,** The most frequent movement sequences made in response to an example configuration during the free search task. The same configuration elicits three different sequences. **d,** Instructed search configurations elicit the same sequence. Probability is shown above each arrow.

[1]Center for Neural Science, New York University, New York, New York 10003, USA. [2]Computation and Neural Systems Program, California Institute of Technology, Pasadena, California 91125, USA. [3]Division of Biology, California Institute of Technology, Pasadena, California 91125, USA.

tasks (Supplementary Materials). We estimated spike–field coherency between spiking in PMd and LFP activity in PRR using a ±150 ms analysis window that was stepped through the trial every 10 ms from before the onset of the search array to the time of the first reach. A highly significant, transient increase in 15-Hz coherence after search array onset was clearly present, as illustrated in an example recording in Fig. 2a. Coherence was significant during both tasks but stronger during free search (Fig. 2b; $P < 0.05$, t-test). Coherence between spiking in PRR and LFP activity in PMd revealed a similar pattern (Fig. 2c, d). In this recording, coherence was only significant during free search and not during instructed search (Fig. 2d).

Significant coherence at 15 Hz implies that the timing of action potentials is correlated with fluctuations in LFP activity. Analysing the relative phase of activity in PMd and PRR supported this and revealed correlations in the timing of activity in each area that were not simply time-locked to search array onset (see Supplementary Results and Supplementary Fig. 4). Interestingly, the amplitude of spike and LFP activity, as opposed to their relative timing, did not predict PMd–PRR coherence. We correlated the strength of the coherence immediately after search array onset with LFP power and did not observe a significant correlation ($P = 0.45$; F-test).

Table 1 | Population PMd spike–PRR field coherence

Centre-out	Free or instructed		
23/221 (10%)	74/314 (24%)		
	Free only	Instructed only	Free and instructed
	31/74 (42%)	20/74 (27%)	22/74 (22%)

Linear regression of spike–field coherence against the change in firing rate immediately after search array onset also revealed that coherence was not simply related to the firing rate ($r^2 = 0.06$, $P = 0.14$). Cells with an increase in firing rate generally had the greatest coherence. However, coherence also increased for some cells whose firing rate decreased or did not change.

Spike–field correlations were present only between select pairs of recording sites. Across the population, 74 PMd spike–PRR field recordings (74/314, 24%) contained statistically significant coherence at 15 Hz after search array onset during either task ($P < 0.05$; t-test; Table 1). A similar proportion of PRR spike–PMd field recordings were significant (43/187, 23%; $P < 0.05$; Table 2). In both cases, spike–field coherence was most prevalent during free search. The fraction of correlated recordings significantly increased between sites with overlapping (less than 20°) response fields ($P < 0.05$; binomial test; 54% of PMd spike–PRR field recordings, 45% of PRR spike–PMd field recordings).

To test whether spike–field coherence between PMd and PRR is specific to decision making, we measured coherence during two control experiments. First, we measured spike–field coherence during a single-target centre-out task, instructing monkeys to move to a single peripheral target. In this task, there was no choice between targets. The proportions of recordings with significant spike–field coherence fell dramatically (Tables 1 and 2). Only 10% (23/221) of PMd spike–PRR field recordings and 9% (13/138) of PRR spike–PMd field recordings had significant coherence. Second, during both search tasks, we found that saccades are reliably made after search array onset (see Supplementary Results). To test whether spike–field coherence was due to these eye movements, we measured coherence in one animal during a variant of the search tasks that involved enforced fixation. Even during fixation, spike–field coherence was significant after search array onset and was strongest during free search (Supplementary Results, Supplementary Fig. 5 and Supplementary Tables 1 and 2). The population average spike–field coherence across all cells recorded during each task reinforced the selectivity for the search tasks (Supplementary Fig. 6). These control experiments demonstrate that spike–field coherence between PMd and PRR is associated with making a decision.

LFP activity was not only correlated with spiking activity in the other area. Within-area spike–field coherence was also significant (Supplementary Results and Supplementary Figs 7 and 8). Because spiking was coherent with locally recorded LFP activity, correlations in LFP activity between areas may capture the correlation we observe. Partial spike–field coherence analysis[16] addresses this concern (Supplementary Methods and Supplementary Fig. 9). In each example recording, partial spike–field coherence remained significant after accounting for local LFP activity ($P < 0.05$, t-test). Significant partial spike–field coherence was also present across the population (74% of PMd spike–PRR field partial coherence and 70% of PRR spike–PMd field partial coherence; see Supplementary Results). Therefore, spike–field coherence between PMd and PRR directly relates the activity of individual neurons with distant LFP activity.

Figure 2 | PMd–PRR spike–field coherence. a, b, Example PMd spike–PRR field coherence: **a**, Time–frequency coherence every 50 ms during free and instructed search. Amplitude is colour coded. Activity is aligned to search array onset (first vertical white bar). Average time of the first reach (second vertical white bar). White horizontal bar shows analysis window for **b**. **b,** Coherence line plot for free (black) and instructed (red) search tasks. Coherence is z-transformed. Significant difference at 15 Hz (**$P < 0.05$; t-test). **c, d,** Example PRR spike–PMd field coherence. **e,** Population average 15 Hz PMd–PRR spike–field coherence every 10 ms. PMd spike–PRR field coherence (solid); PRR spike–PMd field coherence (dashed). Free search (black); instructed search (red). Coherence is z-transformed before averaging; 95% confidence intervals, Bonferroni-corrected (shaded).

Table 2 | Population PRR spike–PMd field coherence

Centre-out	Free or instructed		
13/138 (9%)	43/187 (23%)		
	Free only	Instructed only	Free and instructed
	21/43 (49%)	12/43 (28%)	9/43 (21%)

Spike–field coherence gives two independent measures of the neuronal coordination between PRR and PMd. This may indicate how activity flows across the circuit. We estimated the population average coherence for each of the populations that showed coherence at 15 Hz in either search task and compared them (Fig. 2e). Across each population, PMd-PRR spike–field z-score coherence (see Supplementary Methods) was stronger during free search than instructed search ($P < 0.01$, Bonferroni-corrected t-test). Importantly, PMd spike–PRR field coherence started about 30 ms earlier than PRR spike–PMd field coherence.

Assuming that LFP activity is predominantly synaptic, this suggests that PMd is activated before PRR during search and that PMd spiking is reflected in PRR LFP activity before PRR spiking is reflected in PMd LFP activity (see Supplementary Discussion). The activity is at a relatively low frequency, about 15 Hz, and is transient, about 350 ms. Our time resolution is limited, but the correlation can involve only a few 15-Hz cycles. Because action potentials are propagated between areas, one attractive possibility is that spike–field coherence measures signals in a sub-population of neurons that travel across this circuit first from PMd to PRR and then back from PRR to PMd in a 'handshake'. Consistent with this possibility, the 30 ms latency between the spike–field coherence measurements (Fig. 2e) is a half-cycle at 15 Hz.

PMd and PRR spiking activity lets us examine when each area becomes active. We recorded 115 PMd and 39 PRR neurons responsive to search array onset to measure response latency in each area. PMd spiking responded significantly earlier than PRR spiking in both search tasks (PMd instructed search, 64 ± 6 ms (mean $\pm$ s.e.m.); free search, 79 ± 5 ms. PRR instructed search, 90 ± 10 ms; free search, 109 ± 11 ms; Fig. 3). We then estimated response latency for 110 PMd neurons and 120 PRR neurons recorded in both animals during the centre-out task. PRR cue response latencies were significantly shorter in this task than in either of the search tasks ($P < 0.05$; permutation test); and PMd and PRR response latencies did not differ (PMd, 63 ± 5 ms; PRR, 70 ± 6 ms; $P = 0.51$, Wilcoxon test; Fig. 3e). This suggests that the response latency difference between PRR and PMd is specific to making a decision.

Because spike–field correlations are strongest during decision making, the sub-population of coherent neurons may encode the upcoming movement choice. If so, cells with significant spike–field correlations should predict the movement choice earlier than cells that do not. We analysed this with a receiver-operating characteristic of the firing rate during free search (Supplementary Methods). We calculated the average choice probability separately for correlated and uncorrelated PRR and PMd neurons. In both areas, correlated neurons predict the movement choice after search array onset during the period of greatest spike–field coherence (Fig. 4a, b; see also Fig. 2e). Later in the trial, uncorrelated cells predict the movement choice as accurately as correlated cells. Neurons with long-range correlations may, therefore, exchange information about movement choice between PMd and PRR.

In summary, correlations between PMd and PRR are activated by decision making. Coherence is strongest during free search and is weaker during instructed search. Far less coherence is present during a simpler centre-out task, and the pattern of coherence is unaffected by freely made eye movements. This shows that decision making is distributed across a frontal–parietal circuit and that top-down signals from PMd influence decisions in this circuit.

Why is coherence stronger during free search? This could be due to the nature of the decision. Choices were variable during free search. In contrast, the same choices were made repeatedly during instructed search (Fig. 1). Decision making can be modelled by races underlying the selection of each alternative[17]. These races must be closer during free search because choices are more variable. Therefore, the difficulty of the decision may underlie coherence between PMd and PRR. Cognitive control mechanisms are activated to select between alternative actions. Prefrontal, medial frontal and cingulate cortex are involved in these mechanisms[18–20] and could modulate frontal–parietal coherence during decision making.
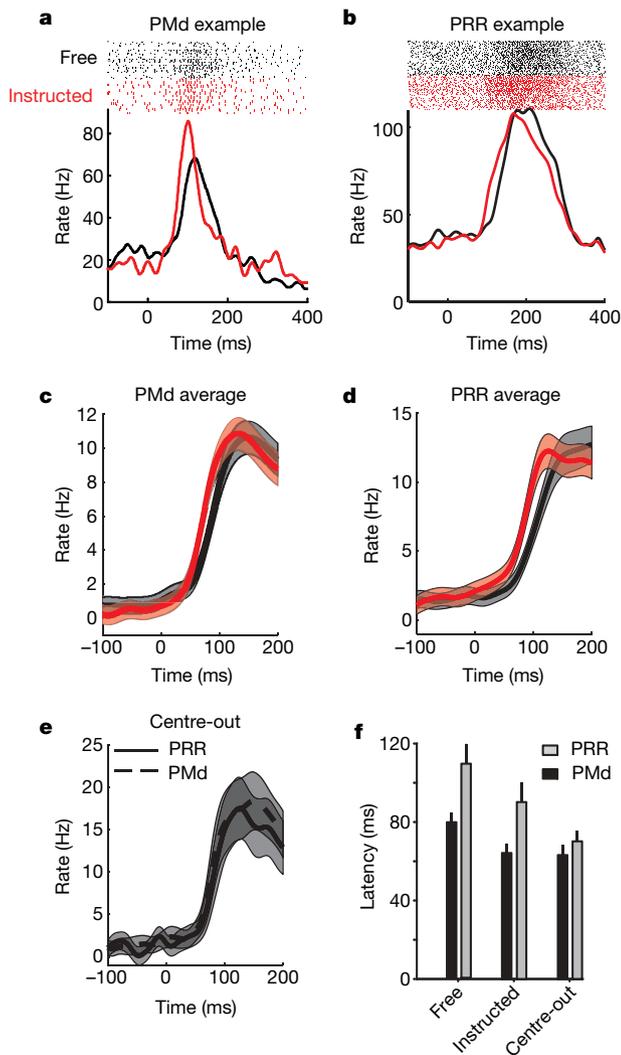
Figure 3 | Spike response latencies. a, Example PMd neuron response to free search (black) and instructed search (red). Activity is aligned to search array onset. Movement to the cell's preferred direction. **b,** Example PRR neuron. **c,** Population average PMd spike response for cells. Activity is baseline subtracted; s.e.m. (shaded). **d,** Population average PRR spike response. **e,** Population average PRR and PMd spike responses during centre-out task to the preferred direction. **f,** Population response latencies for PMd and PRR during free search, instructed search and the centre-out task. Error bars, 95% confidence intervals.
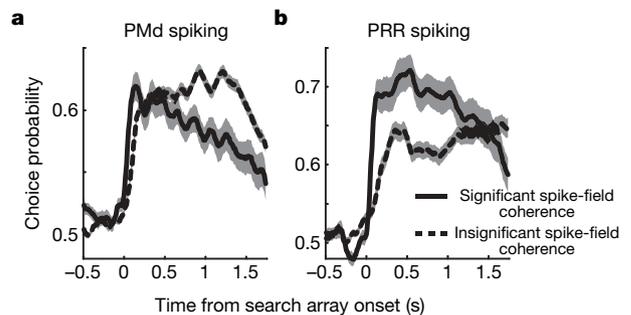
Figure 4 | Receiver-operating characteristic choice probability estimated from the firing rate for neurons with and without significant PMd–PRR spike–field coherence. a, Population average choice probability for correlated (solid) and uncorrelated (dashed) PMd neurons; 95% confidence intervals (shaded). **b,** Same for PRR neurons.

During search, the flow of activity across frontal and parietal cortex may reflect the process of deciding. Information rises fastest in PMd (Fig. 3f), so it cannot be driven by PRR[14] and must take alternative routes, possibly through the thalamus[21]. Information may go from frontal to parietal cortex[22] and then back in a 'handshake' of increased communication (Fig. 2e) that reflects the decision. This transient coordination may reflect how long the decision takes. Subsequent activity may reflect movement planning after the decision (see Supplementary Discussion). Oscillations and synchronization in frontal and parietal cortex exist during attention and movement preparation[4,23–28]. Correlations at specific frequencies could be a signature of these cognitive processes[29]. We have identified a decision circuit in which frontal–parietal communication occurs at relatively low frequencies. The neurons participating in this circuit could play an important role in deciding where to reach.

METHODS SUMMARY

Two male rhesus monkeys (*Macaca mulatta*) participated in the experiments. We recorded single-unit and LFP activity from PMd and PRR using Pt/Ir electrodes controlled by multiple-electrode microdrives (Thomas Recordings). Each monkey was trained to perform a reach search for juice rewards either by freely making choices or by following instructions. Correlations between spiking and LFP activity within and between PMd and PRR were estimated using multitaper spectral methods[4,30]. All surgical and animal care procedures were done in accordance with National Institutes of Health guidelines and were approved by the California Institute of Technology Animal Care and Use Committee.

Full Methods and any associated references are available in the online version of the paper at www.nature.com/nature.

1. Romo, R. & Schultz, W. Neuronal activity preceding self-initiated or externally timed arm movements in area 6 of monkey cortex. *Exp. Brain Res.* **67,** 656–662 (1987).
2. Platt, M. L. & Glimcher, P. W. Neural correlates of decision variables in parietal cortex. *Nature* **400,** 233–238 (1999).
3. Gold, J. I. & Shadlen, M. N. Representation of a perceptual decision in developing oculomotor commands. *Nature* **404,** 390–394 (2000).
4. Pesaran, B., Pezaris, J. S., Sahani, M., Mitra, P. P. & Andersen, R. A. Temporal structure in neuronal activity during working memory in macaque parietal cortex. *Nature Neurosci.* **5,** 805–811 (2002).
5. Sugrue, L. P., Corrado, G. S. & Newsome, W. T. Matching behavior and the representation of value in the parietal cortex. *Science* **304,** 1782–1787 (2004).
6. Cisek, P. & Kalaska, J. F. Neural correlates of reaching decisions in dorsal premotor cortex: specification of multiple direction choices and final selection of action. *Neuron* **45,** 801–814 (2005).
7. Gail, A. & Andersen, R. A. Neural dynamics in monkey parietal reach region reflect context-specific sensorimotor transformations. *J. Neurosci.* **26,** 9376–9384 (2006).
8. Pesaran, B., Nelson, M. J. & Andersen, R. A. Dorsal premotor neurons encode the relative position of the hand, eye, and goal during reach planning. *Neuron* **51,** 125–134 (2006).
9. Quian Quiroga, R., Snyder, L. H., Batista, A. P., Cui, H. & Andersen, R. A. Movement intention is better predicted than attention in the posterior parietal cortex. *J. Neurosci.* **26,** 3615–3620 (2006).
10. Scherberger, H. & Andersen, R. A. Target selection signals for arm reaching in the posterior parietal cortex. *J. Neurosci.* **27,** 2001–2012 (2007).
11. Yang, T. & Shadlen, M. N. Probabilistic reasoning by neurons. *Nature* **447,** 1075–1080 (2007).
12. Johnson, P. B., Ferraina, S., Bianchi, L. & Caminiti, R. Cortical networks for visual reaching: physiological and anatomical organization of frontal and parietal lobe arm regions. *Cereb. Cortex* **6,** 102–119 (1996).
13. Kreps, D. M. *A Course in Microeconomic Theory* Ch. 2 (Princeton Univ. Press, Princeton, 1990).
14. Wise, S. P., Boussaoud, D., Johnson, P. B. & Caminiti, R. Premotor and parietal cortex: corticocortical connectivity and combinatorial computations. *Annu. Rev. Neurosci.* **20,** 25–42 (1997).
15. Mitzdorf, U. Current source-density method and application in cat cerebral cortex: investigation of evoked potentials and EEG phenomena. *Physiol. Rev.* **65,** 37–100 (1985).
16. Halliday, D. M. *et al.* A framework for the analysis of mixed time series/point process data—theory and application to the study of physiological tremor, single motor unit discharges and electromyograms. *Prog. Biophys. Mol. Biol.* **64,** 237–278 (1995).
17. Bogacz, R., Brown, E., Moehlis, J., Holmes, P. & Cohen, J. D. The physics of optimal decision making: a formal analysis of models of performance in two-alternative forced-choice tasks. *Psychol. Rev.* **113,** 700–765 (2006).
18. Goldberg, G. Supplementary motor area structure and function: review and hypotheses. *Behav. Brain Sci.* **8,** 567–616 (1985).
19. Kerns, J. G. *et al.* Anterior cingulate conflict monitoring and adjustments in control. *Science* **303,** 1023–1026 (2004).
20. Daw, N. D. & Doya, K. The computational neurobiology of learning and reward. *Curr. Opin. Neurobiol.* **16,** 199–204 (2006).
21. Schmolesky, M. T. *et al.* Signal timing across the macaque visual system. *J. Neurophysiol.* **79,** 3272–3278 (1998).
22. Cisek, P. Integrated neural processes for defining potential actions and deciding between them: a computational model. *J. Neurosci.* **26,** 9761–9770 (2006).
23. Bressler, S. L., Coppola, R. & Nakamura, R. Episodic multiregional cortical coherence at multiple frequencies during visual task-performance. *Nature* **366,** 153–156 (1993).
24. Murthy, V. N. & Fetz, E. E. Synchronization of neurons during local field potential oscillations in sensorimotor cortex of awake monkeys. *J. Neurophysiol.* **76,** 3968–3982 (1996).
25. Riehle, A., Grun, S., Diesmann, M. & Aertsen, A. Spike synchronization and rate modulation differentially involved in motor cortical function. *Science* **278,** 1950–1953 (1997).
26. Scherberger, H., Jarvis, M. J. R. & Andersen, R. A. Cortical local field potential encodes movement intentions. *Neuron* **46,** 347–354 (2005).
27. Rickert, J. *et al.* Encoding of movement direction in different frequency ranges of motor cortical local field potentials. *J. Neurosci.* **25,** 8815–8824 (2005).
28. Buschman, T. J. & Miller, E. K. Top-down versus bottom-up control of attention in the prefrontal and posterior parietal cortices. *Science* **315,** 1860–1862 (2007).
29. Fries, P. A mechanism for cognitive dynamics: neuronal communication through neuronal coherence. *Trends Cogn. Sci.* **9,** 474–480 (2005).
30. Mitra, P. P. & Pesaran, B. Analysis of dynamic brain imaging data. *Biophys. J.* **76,** 691–708 (1999).

Supplementary Information is linked to the online version of the paper at www.nature.com/nature.

Author Contributions B.P., M.J.N. and R.A.A. designed the experiment and wrote the paper. B.P. and M.J.N. collected the data. B.P. performed the data analysis.

Author Information Reprints and permissions information is available at www.nature.com/reprints. Correspondence and requests for materials should be addressed to B.P. (bijan@nyu.edu).

METHODS

Experimental preparation. Two male rhesus monkeys (*Macaca mulatta*) participated in the experiments. Each animal was first implanted with a head cap and eye coil under general anaesthesia. In a second surgery, recording chambers were implanted in frontal and posterior parietal cortex in the right hemisphere of each animal. Structural magnetic resonance imaging identified the position of the arcuate sulcus and intraparietal sulcus and guided placement of the recording chambers to give access to cortex medial to each sulcus. In both animals, PMd recordings were made within the cortical gyrus within 1.5 mm of the cortical surface, and PRR recordings were made within the intraparietal sulcus 4–9 mm below the cortical surface.

Behavioural tasks. For all tasks, reaches were made with the left arm on a touch-sensitive screen (ELO Touch Systems). Visual stimuli were presented on an LCD display (LG Electronics) placed behind the touch screen. All trials began with the illumination of a central circle which the animal needed to touch with his hand and hold for a baseline period (about 500 ms).

In the search tasks, after a baseline hold period (0.5–1 s), three targets were presented on a 3×3 grid (spaced $10°$) of eight possible locations around the start point. After a delay period (1–1.5 s) the monkey was given a 'go' signal to reach to one of the three targets. Only one of the three targets triggered a juice reward when touched. If the monkey did not reach to the target that gave the reward, he was allowed to make additional reaches to targets after subsequent hold periods (0.5–1 s). Additional reaches were allowed until the reward was received. Targets were extinguished once they were touched. An auditory tone signalled the 'go' signal for each reach. A different set of three targets from the eight possible locations appeared for each trial, and the target that gave the reward was chosen from these three targets with equal probability. This stimulus–reward configuration set ensured that the monkey did not repeatedly perform the same stereotyped sequence of movements. This elicited choices by releasing constraints instead of intensively training the subject to overcome biases and avoid stereotyped choices. If the animal reached for the wrong shape in the instructed search task, the trial was aborted. The animal first knew it was in a free search or instructed search trial when the search array was illuminated.

The free and instructed search tasks were yoked in an interleaved design to match the sensory-, motor- and reward-related contingencies. We did this by requiring the monkey to perform an initial set of free search trials in a block (typically 50). The search array configurations were selected at random from the set of 56 possible configurations. We counted the number of times each search array configuration was presented and the number of times each possible movement sequence was made during the free search task. After the initial set of free search trials was performed, we began to randomly interleave instructed search trials. During this phase of the session, the probability of a given trial being a free search or instructed search task was balanced so that after 200 total trials an equal number of trials from each task would be successfully completed. Search array configurations for the free search task continued to be selected at random. Search array configurations for the instructed search task were drawn from the probability distribution defined by the set of search configurations presented in the preceding free search trials that were successfully completed. To match the motor contingencies in the instructed search trials to the free search trials, the order of the movement sequences instructed by the search array was drawn from a probability distribution defined by the set of movement choices made in the preceding free search trials. To reduce the number of trials needed to estimate these movement sequence probabilities and to prevent the generation of stereotyped movement sequences, we matched only the first element of the instructed movement sequence with the monkey's choices and allowed potential mismatch for the second and third elements of the instructed movement sequence. All probability distributions were updated after each successful trial. Eye movements were unconstrained and, on a subset of experimental sessions (53 sessions in monkey E, 15 sessions in monkey Z), were monitored using a scleral search coil (CNC Engineering).

A variant of the search tasks with enforced fixation was also tested in one animal (monkey E). In this variant, the search tasks were identical except that the monkey needed to maintain fixation at the current touch location throughout the trial. As a result, the only eye movements that were allowed were made at the time of a reach movement.

In the centre-out task, a single target was presented at one of eight peripheral locations on a 3×3 grid (spaced $10°$) around the start point. After a delay period (1–1.5 s) the monkey reached for the target and was then given a juice reward. Fixation was enforced during the period after acquisition of the start point until the end of the delay period. At this time, gaze was unconstrained and both monkeys made a coordinated saccade to the target of the reach movement.